TASK QUARTERLY 10 No 2, 101–112

NUMERICAL ANALYSIS OF THE TIP VORTEX IN AN AIR-CONDITIONER'S PROPELLER FAN

JIABING WANG AND KEQI WU

School of Energy and Power Engineering,
Huazhong University of Science and Technology,
Wuhan, Hubei, 430074, China
hustwjb@163.com

(Received 25 January 2006; revised manuscript received 27 March 2006)

Abstract: A steady, incompressible, turbulent flow field inside a propeller fan used in an air conditioner has been analyzed numerically using the single-equation Spalart-Allmaras turbulence model. It has been found that the formation of tip vortex starts from the blade tip's suction side at about one third of the axial chord's length aft of the rotor's leading edge. It is due to the rolling-up of the intense shear layer flow between the main axial flow and the suck-in inward flow caused by the large pressure difference between the pressure and the suction sides. The tip vortex passes through the blade passage in a curve reversed towards the direction of the blade's rotation. Its trace is partial to the tangential direction as it goes into the aft part of the blade passage covered by the shroud and, simultaneously, its trace in the radial direction is turned from the outward direction to the inward direction. The operating flow rates have an important effect on the axial position of the tip vortex's trace, while its effect on the radial position is negligible. At low flow rates, the vortex disappears at a location closer to the leading edge. The effect of the shroud's width on the tip vortex's trajectory is notable. For a fan with a wide shroud, the trace of the tip vortex moves upstream with a smaller radial influence region than that of a fan with a narrower shroud.

Keywords: tip vortex, internal flow field, propeller fan, numerical simulation

1. Introduction

Low-pressure propeller fans used as cooling fans in air conditioners and automobiles are seldom large in size due to spatial confines. However, the requirements for low noise and high performance of these systems have recently been increasing. Thus, a better understanding of their internal flow characteristics has become necessary to achieve higher fan performance.

Many researchers have attempted to identify the complicated flow mechanism inside axial turbine machinery, most of them focused on fully-ducted compressors and fans. However, low-pressure propeller fans used in outdoor units of split room air conditioners have a special configuration, in which the shroud covers only the rear region of the rotor tips, just as in half-ducted axial flow fans. Moreover, the rotors of these fans are always designed to produce large forward sweep and a forward

curved vane, in order to reduce the noise. The resulting flow inside the fan has its distinguishing characteristics, especially in the rotor tip region.

Three-dimensional vortical flow in the rotor tip region is closely related to fans' performance and noise characteristic. In the early 1990's, Fukano *et al.* [1, 2] investigated systematically the effect of the axial position of a propeller fan relative to the shroud, the shroud's width, the shape of the shroud's inlet and the tip clearance on fans' performance and established the optimum conditions for a low noise propeller fan. Sato and Kinoshita [3] implemented a Laser Doppler Velocimeter (LDV) technique to measure the flow pattern around a propeller fan and discovered that the flow pattern near the rotor tip around the shroud inlet was related to the shape of the shroud and the air volume's flow rate. The separated flow at the inlet edge of the fan shroud at the design point and the inlet reverse flow hindering the inflow entering the blade tips in the small air volume region impair fans' aerodynamic and aero-acoustic performance. Sato and Kinoshita pointed out that a fan's noise could be reduced by optimization of the shroud's shape. Revised shroud configuration was considered in order to reduce the noise level in the experimental work of Akaike and Kikuyama [4]. Later, in addition to the LDV experiment, Jang *et al.* [5–8] examined the flow structure of three-dimensional vortices and their unsteady nature in the rotor tip region using the Large Eddy simulation, which indicated that the tip vortex plays a major role in the structure and unsteady behavior of the vortex flow in propeller fans. Moreover, the vortical flow causes high-pressure fluctuation on the blades' surface. Jang *et al.* demonstrated that a fan's noise could be reduced by controlling the behavior of the vortical flow near the rotor tips with optimization of the shroud's shape. More recently, Cai [9] performed velocity measurements with a two-component LDV system, examining the tip vortex's structure and behavior in an axial fan with no casing wall. As vortices' flow in the tip region has a considerable effect on fans' noise, many measures have been proposed to improve fan performance. Longhouse [10] found that attaching rotating shrouds to rotor tips was a practical method of controlling tip clearance noise. Using the particle image velocimetry (PIV) technique, Nashimoto *et al.* [11] studied the aerodynamic noise and the vortex flow field in an automobile cooling fan with and without winglets on the fan blades under actual operating conditions. They found that installing winglets could change the development and trace of the tip vortex, thus reducing aerodynamic noise.

Most of the earlier research on propeller fans has been experimental. However, the tip vortex has a large turbulent structure, suitable for a CFD technique to be applied in order to examine its flow patterns.

Therefore, the objective of this study is to provide further physical insight into the vortical flow phenomena occurring in propeller fans and better understand the tip-vortex feature. A numerical simulation has been carried out with the FLUENT commercial CFD code. The internal flow field of a propeller fan used in the outdoor unit of split room air conditioners has been obtained, based on which the formation and the development of the tip vortex is shown.

2. The fan's configuration

A sketch of the propeller fan used in the present study is shown in Figure 1. The inflow region consisted of a front and a side inlet; however, the fan's driving motor, the upstream heat exchanger and the downstream grille have been ignored here for the sake of computational convenience.

The fan had a design flow coefficient of 0.27 and a design static pressure rise coefficient of 0.1. Non-dimensional parameters, *i.e.* flow coefficient ϕ and static pressure rise coefficient ψ, were defined as follows:

$$\phi = \frac{4Q}{\pi (D_t^2 - D_h^2) U_t}, \tag{1}$$

$$\psi = \frac{2\Delta P_s}{\rho U_t^2}, \tag{2}$$

where Q was the volume flow rate, ΔP_s was the static pressure rise, D_t was the rotor tip's diameter, D_h was the inlet rotor hub's diameter, U_t was the peripheral velocity at the rotor tip, and ρ was the density of air. The rotor was of meridian acceleration flow type with a hub inclination of 18.4° and a tip inclination of 0°. It had three blade numbers and its tip's diameter was 404mm, with the inlet hub/tip ratio of 0.297. The rotational speed of the rotor was 910rpm. Notably, the shroud was near the trailing edge of the rotor, whose inner diameter was 412mm and width – 67mm. Thirty percent of the axial chord's length at the rear part of the rotor's tip section was covered by the shroud. The rotor tip clearance was 4mm. The Reynolds number based on the rotor tip's peripheral velocity and its chord length was $4.2 \cdot 10^5$.

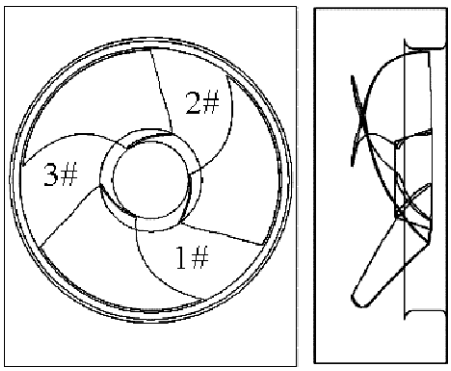

Figure 1. Schematic view of the propeller fan

3. The numerical method

A fully implicit, segregated finite-volume method solving three-dimensional Reynolds-averaged Navier-Stokes viscous partial differential equations was used in the numerical calculations to study the propeller fan's internal flow field. The single-equation Spalart-Allmaras turbulent model was used for the purpose of turbulence closure, a model popular among CFD researchers [12]. The flow was assumed to be steady and incompressible. The second-order upwind difference scheme was employed to spatially discretize the convection terms. The pressure-velocity coupling was handled using the SIMPLE algorithm.

4. The computational grids and boundary conditions

An unstructured grid was generated because of the complex computational domain of an axial flow fan. Compared to other regions, the grid of the blade region, being the main region of energy transference, had a higher grid density due to steep gradients of the flow properties.

In the current simulation, the inflow boundary and the outflow boundary were defined as pressure boundary conditions, where atmosphere and specified static pressure were given respectively. The impeller's wall was defined as a moving wall with a rotating frame of reference, while other walls were defined as stationary walls in an inertial frame of reference. A no-slip boundary condition was used on the solid walls. The convergence criterion was set at 10^{-3} for the residual numbers.

5. Results and discussion

The predicted flow rate coefficient of the present numerical simulation was approximately equal to 0.27 at the design static pressure rise coefficient of 0.1, which was in good agreement with the experimental coefficient, thus validating the numerical results.

The vortical flow characteristic in the rotor tip region yielded by the presented simulation results is discussed in the following subsections. It should be born in mind that the following analysis refers to the design flow coefficient, except where specifically stated otherwise.

5.1. Formation of the tip vortex

Streamlines of various meridian sections are shown in Figure 2. The location of each meridian section has been arranged at intervals of 6 degrees along the circumferential direction from the blade suction surface to the adjacent pressure surface, as shown in Figure 4. So, in the present fan model, the leading edge of a blade's tip is located in the section of pitch = 0 and pitch = 1, while the trailing edge of the tip is located in the section of pitch = 0.7 and pitch = 1.7. Near the blade tip, *viz.* from the meridian section of pitch = 0 to that of pitch = 0.1, where the pressure difference between the pressure surface and the suction surface sides is small, an inward radial flow is induced, as the shroud is absent there (Figures 2a and 2b). From the meridian section of pitch = 0.15 to pitch = 0.3, the fluid near the suction side maintains the inward radial flow, while the fluid near the pressure side has been turned to the outward radial flow, as the pressure there has gradually increased due to the Coriolis force and the centrifugal force generated by the rotor rotation, as shown in Figures 2c and 2d. Simultaneously, the pressure difference between the pressure side and the suction side has gradually increased. Then, in the meridian section of pitch = 0.45, the fluid near the blade tip's pressure side flows towards the suction side, which results in stream-wise curving on the suction surface side. So, the vortex is generated due to rolling-up of the intense shear layer flow between the main axial flow and the suck-in inward flow near the suction side (see Figure 2e). Thereafter, the tip vortex develops, with its volume gradually increasing and its center departing from the suction surface (see Figure 2f). The tip vortex has the largest volume when it is just upstream of the shroud (see Figure 2g). Subsequently, due to the influence

of the shroud, the tip vortex is gradually removed away from the suction surface and moves inside the shroud, with its volume diminished and its shape changed (see Figures 2h to 2j). Meanwhile, the fluid in front of the shroud is again turned into an inward radial flow after the tip vortex has moved inside the shroud completely, as shown in Figure 2i. Finally, the tip vortex disappears about the meridian section of pitch = 1.55 (see Figure 2k). From the meridian section of pitch = 1.6 to pitch = 1.9, no vortex can be observed in the flow passage (*cf.* Figure 2l).

The above analysis implies that the fluid flowing into the blade passage includes not only the axial inflow through the rotor's leading edge region, but also the inward radial inflow through the fore part of the rotor's tip. Undoubtedly, this flow pattern is determined by the special configuration of the shroud. The tip vortex is induced by the rolling-up of the shear flow, owing to the large pressure difference between the pressure and the suction sides. The onset of the tip vortex is located on the blade tip's suction side, at about one third of the axial chord's length aft of the rotor's leading edge. It then forms a large reverse flow region upstream of the shroud, where the outward radial flow distributed from the meridian section of pitch = 0.3 to pitch = 0.6 occupies up to about thirty percent of the circumferential flow passage in the tip region. Calculations have shown that there is relatively high stream-wise absolute vorticity near the tip-vortex position. The mainstream with large axial velocity is under the tip vortex.

5.2. Trajectory of the tip vortex

A major source of efficiency lost in turbo-machinery rotors is the secondary loss due to secondary flow. Secondary flow is believed to be mainly caused by stream-wise absolute vorticity, *i.e.* the component of absolute vorticity along the relative flow direction.

Stream-wise absolute vorticity, ξ_s, and normalized helicity, H_n, are very useful to understand the vortex structure and have been used in many references [6, 7, 9]. Having obtained the velocity vector field, the two non-dimensional parameters can be calculated as follows:

$$\xi_s = \frac{\vec{\xi} \cdot \vec{w}}{2\omega |\vec{w}|} = \frac{\xi_r \cdot w_r + \xi_\theta \cdot w_\theta + \xi_z \cdot w_z}{2\omega \sqrt{w_r^2 + w_\theta^2 + w_z^2}}, \tag{3}$$

$$H_n = \frac{\vec{\xi} \cdot \vec{w}}{|\vec{\xi}| \cdot |\vec{w}|} = \frac{\xi_r \cdot w_r + \xi_\theta \cdot w_\theta + \xi_z \cdot w_z}{\sqrt{\xi_r^2 + \xi_\theta^2 + \xi_z^2} \cdot \sqrt{w_r^2 + w_\theta^2 + w_z^2}}, \tag{4}$$

$$\vec{\xi} = \nabla \times \vec{V} = \xi_r \vec{i}_r + \xi_\theta \vec{i}_\theta + \xi_z \vec{i}_z, \tag{5}$$

where ω is the angular velocity of the rotor, $\vec{\xi}$ is the absolute vorticity calculated with formula (5), while $\vec{w}$ and $\vec{V}$ respectively denote relative and absolute flow velocity. Stream-wise absolute vorticity is normalized by twice the angular velocity of the rotor, wherefrom the decay of vorticity in the streamwise direction can be investigated; it is therefore used to locate the vortex's position and its rotation direction. Normalized helicity is the cosine of the angle between the absolute vorticity and the relative velocity vectors, the magnitude of which tends to unity in the vortex's core, with its sign indicating the vortex's swirl direction relative to the stream-wise velocity component. In contrast to stream-wise absolute vorticity, distributions of normalized

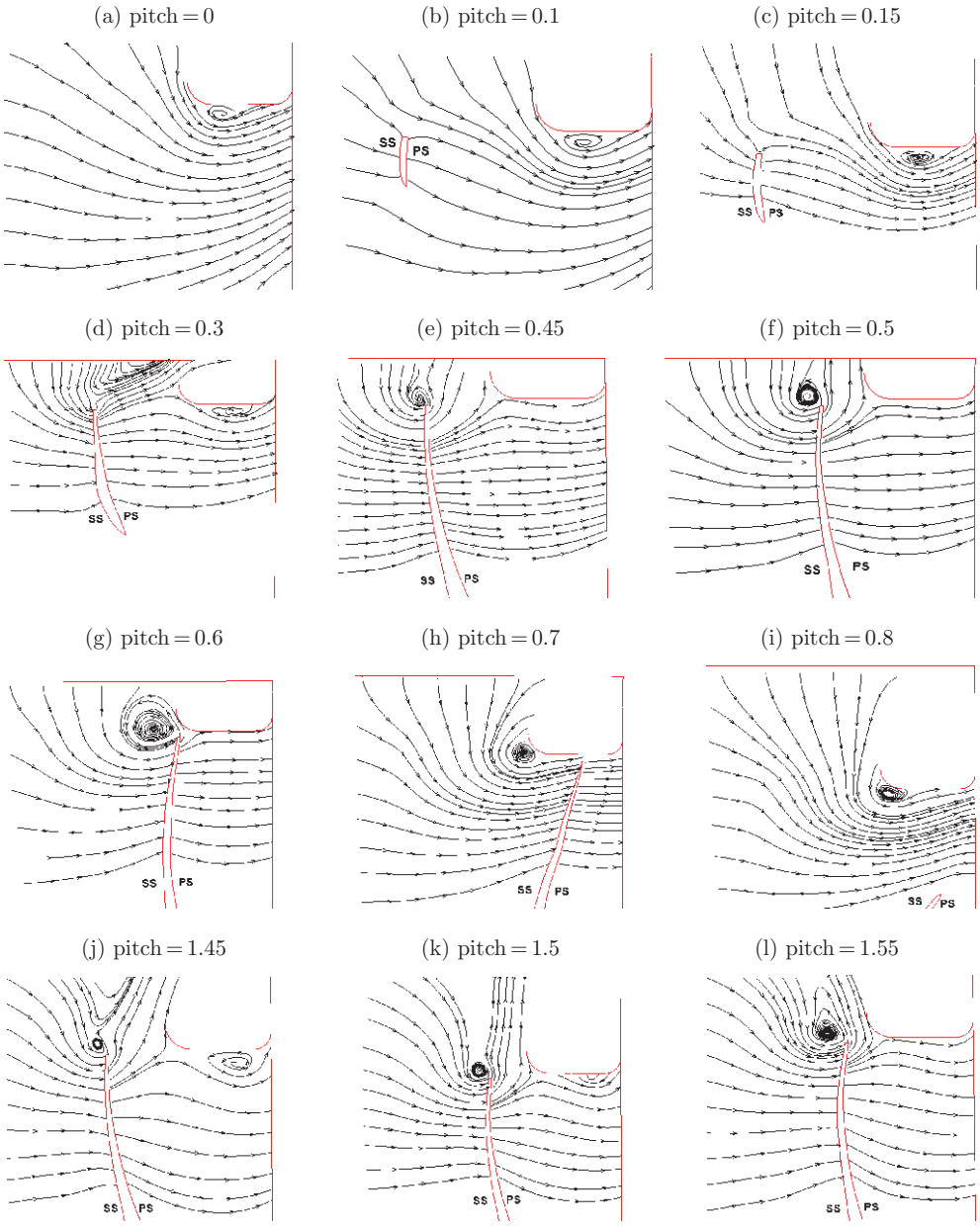

Figure 2. Tangential distribution of meridian streamlines

helicity along the vortex core allow us to analyze the change in the vortex's nature quantitatively, regardless of the decay of vorticity in the stream-wise direction [7].

The distribution of stream-wise absolute vorticity near tip region is shown in Figure 3. The high stream-wise absolute vorticity visible in the figure as a red region marks the trajectory of the tip vortex. The tip vortex appears on the suction side near the leading edge of the rotor's tip and passes through the blade passage in

a curve reversed towards the blade's rotation direction. Near the rotor's trailing edge, stream-wise absolute vorticity is reduced, which marks the decay of absolute vorticity in the stream-wise direction.

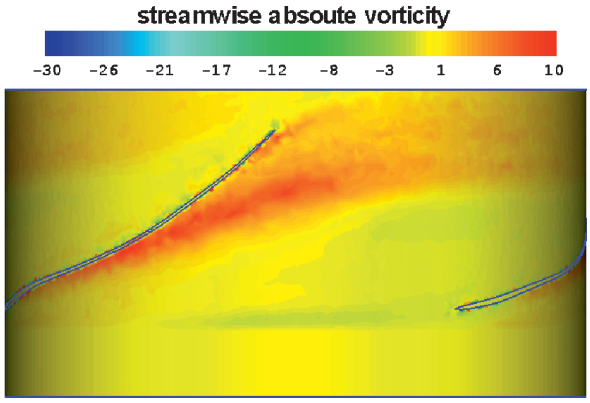

Figure 3. Distribution of stream-wise absolute vorticity near the tip region

The trajectory of the tip vortex at various circumferential positions is shown in Figure 4. The tip vortex's position is determined by the position of minimum kinetic energy in each meridian section. A similar tip vortex's trace trend is found at various circumferential positions, although there are some differences in the vortex's onset and the distances traveled along the axial, circumferential and radial directions, due to the asymmetrical configuration of the fan system and the inflow conditions. This implies that the tip vortex has a relative movement in its rotational process. The trace of the tip vortex shown in Figure 4a resembles a curve which is partial to the tangential direction as it moves into the aft part of the blade passage covered by the shroud. Actually, the movement of the tip vortex is gradually enhanced in the tangential direction and weakened in the axial direction when it enters the rotor exit. While there, it located at about seventy-five percent of the circumferential distance between the blade passage and the trailing edge at the suction side. Finally, the tip vortex disappears at about four percent of the axial chord's length of the blade tip. The trajectory of the tip vortex along the radial direction is shown in Figure 4b. At the onset, the vortex's radial position is slightly in excess of the rotor tip's radius. Then, the tip vortex moves outwards towards greater radii, until it is just upstream of the shroud. At that moment, it reaches its maximum radial position, about three percent greater than the rotor tip's diameter. Subsequently, the vortex moves inwards towards lower radii, due to the influence of the shroud. Its radial location is below the rotor tip's diameter after the meridian section of pitch > 0.8 and reaches its lowest radial location at the meridian section of pitch $= 1.3$. Thereafter, the tip vortex core moves in the outward radial direction and finally disappeared. The trace of the tip vortex is thus closely related to the position of the shroud relative to the rotor.

The trajectory of the tip vortex described above almost results in a vortex ring in the rotor tip region, as shown in Figure 5, which would obviously have a considerable blocking effect on the underside main flow. The path lines surrounding the tip vortex's core are shown in Figure 6. The magnitude of normalized helicity in the

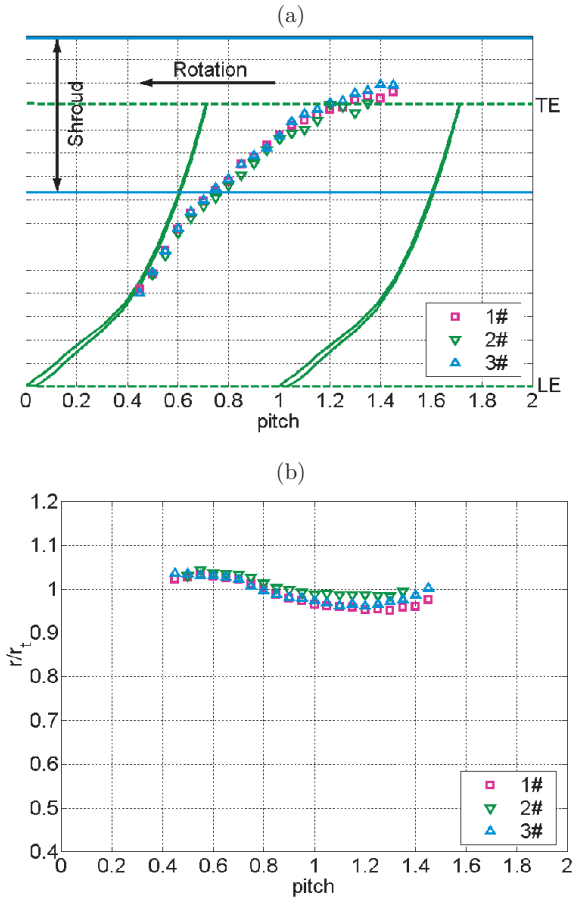

Figure 4. Trajectory of the tip vortex

tip vortex's core region tends to 1 throughout the vortex's trace (*cf.* Figure 7a), which indicates that the vortex has not significantly changed its nature during the whole development process with its swirl direction along the direction of the stream-wise velocity component, as it has not impinged on the pressure surface of the adjacent blade. Stream-wise absolute vorticity has a large value near the suction surface and then gradually decreases along the trace of the tip vortex until it becomes very small near the pressure surface (see Figure 7b). This corresponds to the tip vortex being generated near the suction surface and disappearing near the pressure surface due to the complex effect of viscosity diffusion and turbulence. The flow of the tip vortex gradually decelerates during the development process, which is implied by the distribution of relative velocity's magnitude along the tip vortex core (see Figure 7c).

The above calculated results are partially similar to the results of reference [6]. However, in that reference the tip vortex convects nearly in the tangential direction and impinges on the pressure surface near the tip of the adjacent blade, what results in an abrupt change in its nature indicated by the rapid change in the magnitude of normalized helicity from 1 to -1. Presumably, the difference between these results is due to the lower pressure head and fewer blades applied in the present propeller fan.

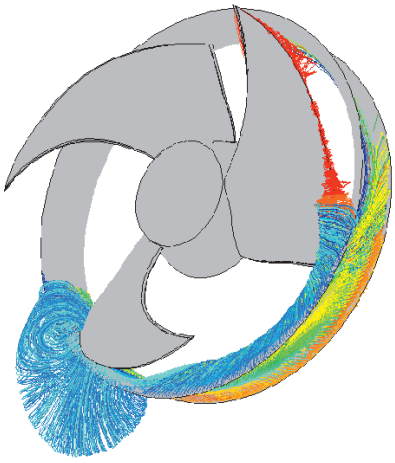

Figure 5. The tip vortex ring

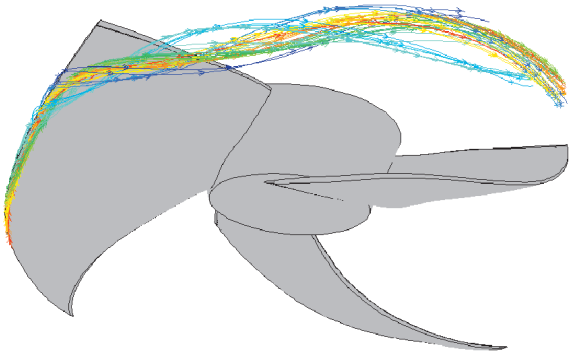

Figure 6. Path lines surrounding the tip vortex core

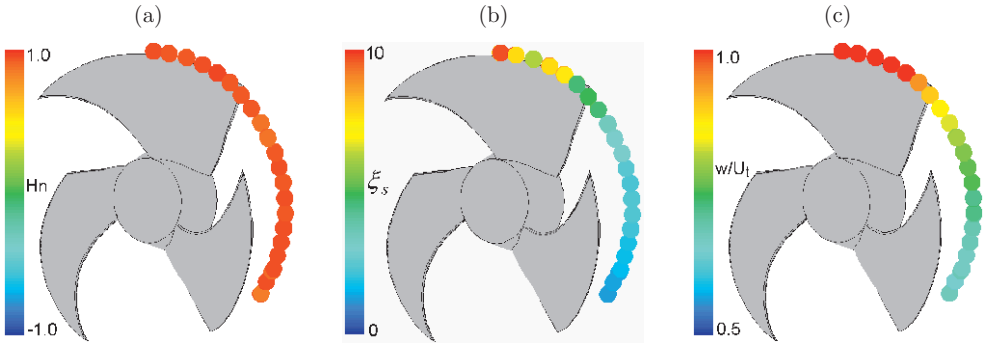

Figure 7. Trajectory of the tip vortex core colored for (a) normalized helicity, (b) stream-wise vorticity and (c) relative velocity

5.3. Effect of flow rates on the tip vortex's trajectory

The trajectory of the tip vortex under various flow rate conditions is shown in Figure 8, where DQ means the design flow coefficient of 0.27, HQ is the high flow coefficient of 0.30, and LQ is the low flow coefficient of 0.23. The flow rates have an important effect on the axial position of the tip vortex, especially on its axial position

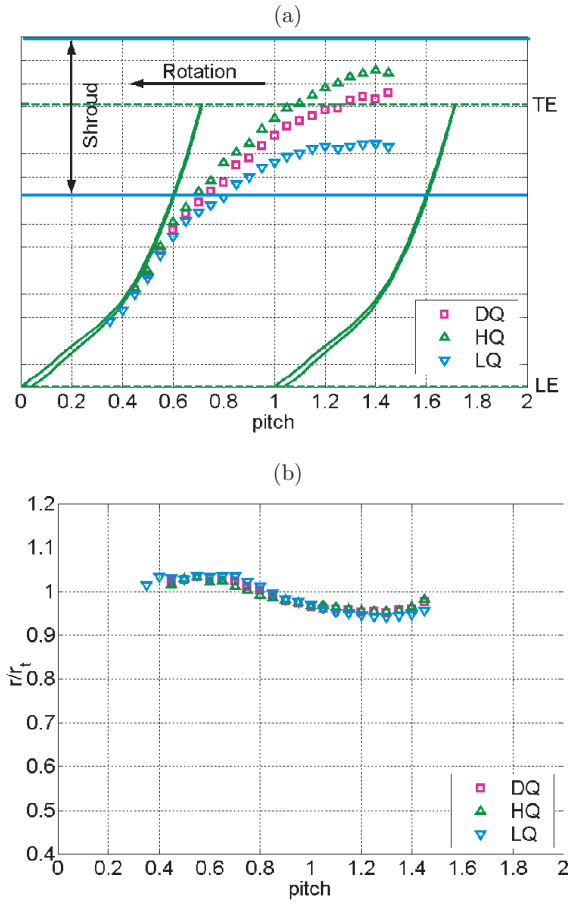

Figure 8. Trajectory of the tip vortex under various flow rate conditions

in the aft part of the flow passage, while their effect on the radial position of the vortex is negligible. At low flow rates, the tip vortex's movement along the axial direction is much weaker, so that it disappears at a location closer to the leading edge, still inside the blade passage. The axial velocity is greater at high flow rates, so that the vortex disappears downstream of the rotor exit. The vortex disappears at almost the same circumferential location under various flow rate conditions.

5.4. Effect of the shroud's width on the trajectory of tip vortex

The tip vortex's trajectory in propeller fans of varying shroud width is shown in Figure 9 at the flow coefficient of 0.27. "CR" means the percentage ratio of the axial chord's length at the rear part of the rotor's tip section covered by the shroud to the rotor tip's axial chord. The relative axial position of the shroud's exit and the rotor remain identical under all calculated conditions. So, a fan with a wide shroud must have a high CR ratio. The trajectory of the tip vortex is clearly related to the width of the shroud. The onset and disappearance position of the tip vortex with varying shroud width are nearly identical, but its trace in the flow passage differs. For a fan with a wide shroud, the trace of the tip vortex moves upstream, while it moves downstream for a fan with a narrow shroud. The tip vortex region is smaller

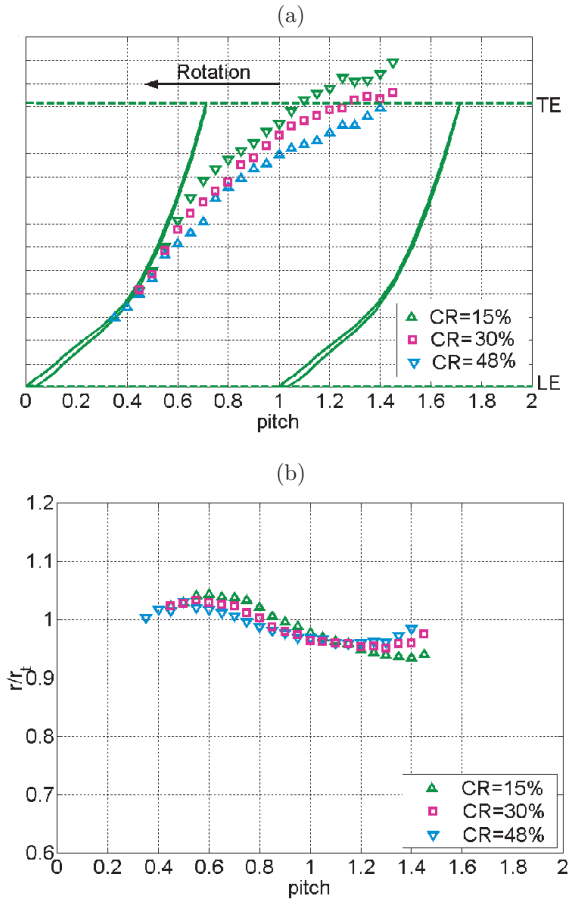

Figure 9. Trajectory of the tip vortex at various shroud widths

along the radial direction in a wide-shrouded fan than in a narrow-shrouded fan. It is so because the development of the tip vortex along the radial direction is mainly completed upstream of the fan shroud, as can be seen in Figure 4b. Once the vortex enters the flow passage covered by the shroud, the shroud suppresses its development along the radial direction. Thus, a wide shroud results in a small radial region of the tip vortex.

6. Conclusions

Three-dimensional numerical analysis of the viscous turbulent flow field of a propeller fan with a shroud covering the rear region of the rotor tips has been implemented successfully. The calculated results provide a comprehensive understanding of the vortex flow pattern in the fan's blade tip region.

1. The fluid flow into the blade passage includes not only the axial inflow through the rotor's leading edge region, but also the inward radial inflow through the fore part of the rotor's tip.
2. Formation of the tip vortex starts from the blade tip's suction side at about one third of the axial chord's length aft of the rotor's leading edge, due to

rolling-up of the intense shear layer flow between the main axial flow and the suck-in inward flow caused by the large pressure difference between the pressure and the suction sides. It disappears near the rotor's exit without impinging on the pressure surface of the adjacent blade.

3. The tip vortex passes through the blade passage in a curve reversed towards the blade's rotational direction. Its trace is partial to the tangential direction as it enters the aft part of the blade passage covered by the shroud and, simultaneously, its trace in the radial direction turns from the outward to the inward direction. The tip vortex's trajectory nearly results in a vortex ring in the rotor tip region.
4. The operating flow rates have a significant effect on the axial position of the tip vortex's trace, while its effect on the radial position is negligible. At lower flow rates, the tip vortex disappears at closer to the leading edge.
5. The effect of the shroud's width on the tip vortex's trajectory is notable. For a fan with a wide shroud, the trace of the tip vortex moves upstream, while it moves downstream for a fan with a narrow shroud. The tip vortex region is smaller along the radial direction in a fan with a wide shroud than in a fan with a narrow shroud.

Acknowledgements

The project was partially supported by the National Science Foundation of China (grant no. 50176012), most gratefully acknowledged by the authors.

References

[1] Fukano T, Fukuhara M, Kawagoe K, Hara Y and Kinoshita K 1990 *Trans. JSME* **B 56** 3378 (in Japanese)
[2] Fukano T, Kawagoe K, Fukuhara M, Hara Y and Kinoshita K 1990 *Trans. JSME* **B 56** 3383 (in Japanese)
[3] Sato S and Kinoshita K 1993 *The 4th Asian Int. Conf. on Fluid Machinery*, Suzhou, Peoples R China, pp. 166–170
[4] Akaike S and Kikuyama K 1993 *Trans. ASME J. Vib. Acoust.* **115** (2) 216
[5] Jang C M, Furukawa M and Inoue M 2001 *JSME Int. J.* **B 44** (4) 748
[6] Jang C M, Furukawa M and Inoue M 2001 *Trans. ASME, J. Fluids Eng.* **123** (12) 748
[7] Jang C M, Furukawa M and Inoue M 2001 *Trans. ASME, J. Fluids Eng.* **123** (12) 755
[8] Jang C M, Furukawa M and Inoue M 2003 *JSME Int. J.* **B 46** (1) 163
[9] Cai W X 2001 *Behavior of Tip Vortices in Diagonal Flow Fan and Open Axial Fan*, Dissertation, Saga University
[10] Longhouse R E 1978 *J. Sound Vib.* **58** (2) 201
[11] Nashimoto A, Fujisawa N, Akuto T and Nagase Y 2004 *J. of Visualization* **7** (1) 85
[12] Han C, Tsung F L and Loellbach J 1998 *JSME Int. J.* **B 41** (1) 200